Lawrence Berkeley National Laboratory

Title

Electronic Tuning of Mixed Quinoidal-Aromatic Conjugated Polyelectrolytes: Direct Ionic Substitution on Polymer Main-Chains

Permalink

https://escholarship.org/uc/item/7b8462bd

Journal

ISSN

Authors

Anderson, Christopher L
Dai, Nan
Teat, Simon J
et al.

Publication Date

DOI

Peer reviewed

Electronic Tuning of Mixed Quinoidal-Aromatic Conjugated Polyelectrolytes via Direct Ionic Substitution

Christopher L. Anderson,[†,‖] Nan Dai,[#] Simon Teat,[§] Bo He,[†,‡] Shu Wang,[#] Yi Liu[†,‡*]

†The Molecular Foundry, ‡Materials Sciences Division, and §Advanced Light Source, Lawrence Berkeley National Laboratory, One Cyclotron Road, Berkeley, California 94720, United States

‖Department of Chemistry, University of California, Berkeley, Berkeley, California 94720, United States

#Laboratory of Organic Solids, Institute of Chemistry, Chinese Academy of Sciences, Beijing 100190, P. R. China

ABSTRACT: We introduce the direct ionic substitution strategy of generating strongly electron-accepting ionic motifs and showcase its utility by synthesizing and characterizing a series of ionic azaquinodimethane (iAQM) compounds. The facile introduction of cationic substituents onto the quinoidal para-azaquinodimethane (AQM) core gives rise to a strongly electron-accepting building block, which can be readily employed in the synthesis of ionic small molecules and conjugated polyelectrolytes (CPEs). A succinct synthesis utilizing low-cost reagents affords a wide variety of functionality in these mixed aromatic-quinoidal systems that are otherwise difficult to access. Electrochemical measurements alongside theoretical calculations indicate notably low-lying LUMO values for the iAQM species. The optical band gaps measured for these compounds are highly tunable based on structure—ranging from 2.30 eV in small molecules down to 1.22 eV in polymers. The iAQM small molecules and CPEs showcase the effects of combining the donor-acceptor strategy and the bond-length alternation reduction strategy of band gap reduction. To make use of their notable optical properties, the application of the iAQM CPEs as active agents in photothermal therapy was also demonstrated.


Introduction

Conjugated polyelectrolytes are a class of polymeric organic materials featuring conjugated backbones with pendent ionic groups.[1-15] These features imbue CPEs with high polarity and crystallinity as well as the semiconducting properties. CPEs are also unique amongst conjugated polymers in that they are more likely to exhibit amplified fluorescence quenching effects, are capable of forming unique structures through layer-by-layer deposition, and in some cases, may exhibit the ability to self-dope.[2-7] The unique properties of CPEs have led to their extensive use in optoelectronics, sensing, and imaging applications.[3-9,16] CPEs are also being utilized as active materials in novel device architectures incorporating both ionic and electronic conduction—a necessary combination of properties in some neuromorphic computing and bioelectronics applications.[10,11,16-18]

Photothermal therapy (PTT) is a proposed method of treating various health maladies including antibacterial-resistant infections and cancer.[5,12,13,19-21] PTT makes use of an active chemical agent that absorbs light and dissipates the energy as heat. Gold nanoparticles and carbon allotropes have most extensively been explored as the active agents in PTT, but both suffer from the lack of any known metabolic breakdown pathway and are thus assumed to be deleterious over long periods of time.[21] Conjugated polymers are well-suited for use as active agents in photothermal therapy due to their relatively large molar absorption coefficients, good photostability, and the possibility of their biodegradability.[19,20] NIR absorbance in photothermal agents allows for access deeper into tissue, and a lack of fluorescence in an anoxic environment indicates that nonradiative relaxation pathways are prominent.[5,19-21] CPEs may be uniquely suited for use as photothermal agents due to the possibility for their water-solubility and—given positively charged side-chains—their ability to adhere to bacterial membranes.[5,12,13] Still, there are few examples of CPEs being used for photothermal therapy.[12]

In many CPEs, the ionic substituents are situated on the ends of pendant alkyl chains, and are thus spatially separated from the conjugated main chain (Scheme 1a).[1-11,15] The

electronic properties of CPEs are then primarily determined by the main chain structure, while the ionic groups have only marginal effects on the electronics. There have been a small number of examples in which carboxylate or sulfonate groups are directly attached to the main chain of a CPE, but no exploration of the electronic effects of the ionic substitution was undertaken in these cases.[7,14,15,22,23] Direct bonding of ionic groups to the polymer main chain in CPEs represents an effective strategy to tune the electronic structures of CPEs, however it remains largely unexplored, possibly due to the lack of suitable conjugated ionic building blocks (Scheme 1a).

Scheme 1. (a) Illustration of two different types of CPEs; (b) structural diagram of the dicationic iAQM as a building block for CPEs (Nu: neutral nucleophiles such as pyridine, triphenylphosphine, etc.)
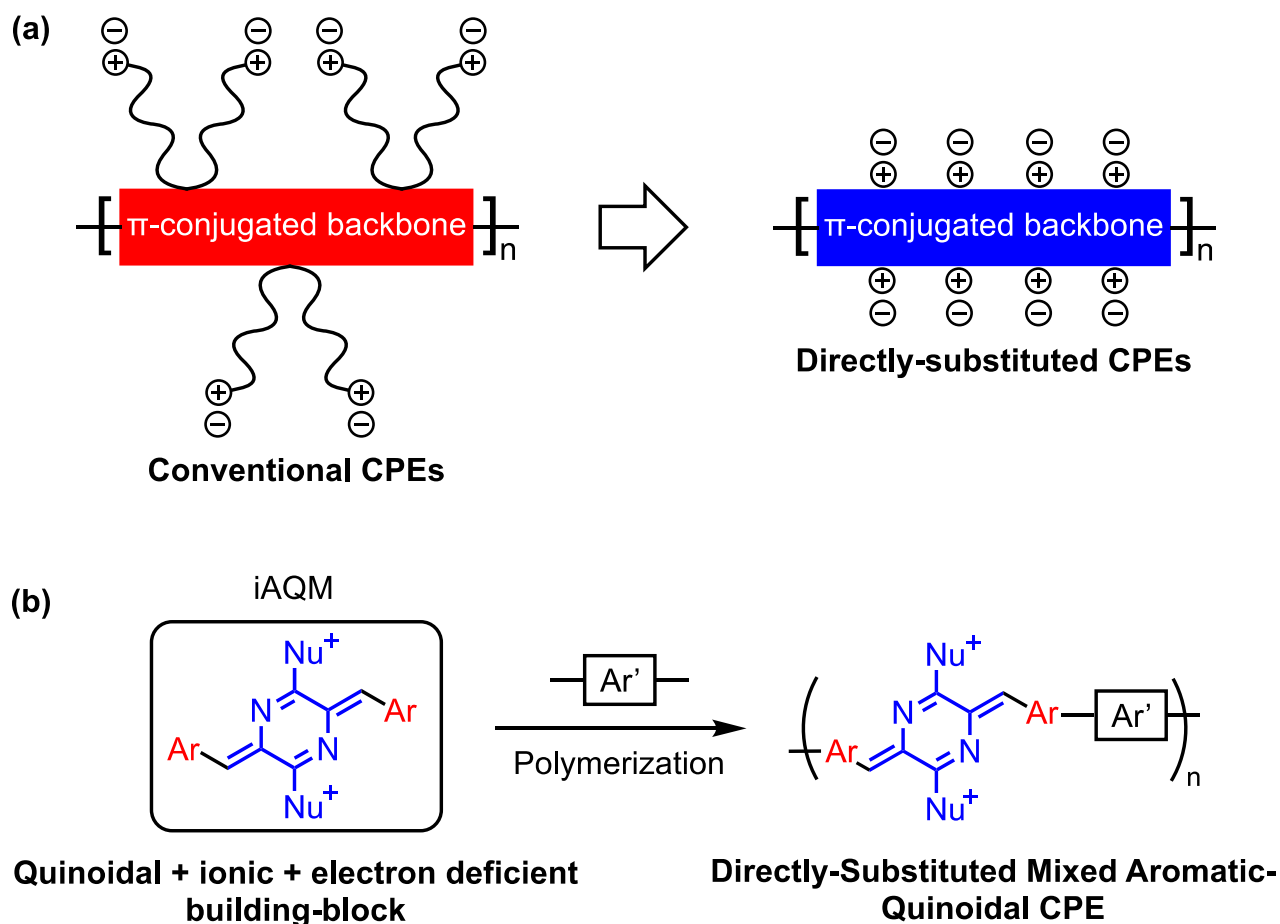
For many of the applications of CPEs, it is necessary to have control over both the size of the band gap and the frontier molecular orbital (FMO) energy levels. The direct conjugation

of electron-donating and accepting groups has been a widely used strategy to rationally tune the band gaps of conjugated polymers to date.[24-27] However, the incorporation of quinoidal building blocks into otherwise aromatic conjugated polymers represents a complementary band gap reduction strategy.[27-30] The reduction in bond-length alternation (BLA) accompanying the introduction of quinoidal units into a conjugated polymer destabilizes its electronic ground state and stabilizes its excited states in a relative sense, reducing the band gap while also increasing the effective conjugation length.[25,27-31] The combination of the mixed donor-acceptor strategy with the BLA reduction strategy represents a powerful combination for the reduction in band gap, while also allowing for more freedom in the overall electron donating or accepting character of the polymer.[27-30]

Perhaps the simplest quinoidal building block that could be incorporated into a conjugated polymer would be the quinoidal analog of benzene—also known as *para*-quinodimethane (*p*-QM). *p*-QM and its nitrogen-substituted analog, 2,5-dimethylene-2,5-dihydropyrazine (DDHP), are highly reactive quinoidal molecules that spontaneously polymerize under ambient conditions, restricting their incorporation into conjugated polymeric systems.[32] Recently, the synthesis of the *para*-azaquinodimethane (AQM) motif—a DDHP derivative—was detailed.[33] Notably, these AQMs are stable under both ambient atmospheric conditions and standard organic chemical handling, permitting one of the simplest quinoidal building blocks to be incorporated into conjugated polymers that were shown to display high mobilities in organic field-effect transistor architectures.[33]

The ionic azaquinodimethane compounds described herein showcase the electronic effects of direct substitution of a quinoidal DDHP core with ionic groups (Scheme 1b). The direct ionic substitution of the AQM ring yields strongly electron-withdrawing moieties with small, highly tunable band gaps that can be further incorporated into conjugated polyelectrolytes. These ionic and conjugated building blocks are soluble in polar organic

solvents, and are stable to further chemical modification. The iAQM-based CPEs so generated show absorbances reaching into the NIR, displaying the efficacy of combining the donor-acceptor strategy with the BLA reduction strategy in the design of conjugated polymeric materials.[26,33,34]

Results and Discussion

Materials Synthesis

As shown in Scheme 2, Knoevenagel condensation of various aryl aldehydes **2a-c** with 1,4-diacetyl-2,5-diketopiperazine (**1**) afforded 2,5-diarylidine-3,6-diketopiperazine-diones **3a-c**.[35] Attempts to generate activated intermediates from **3a-c** using phosphorous(V) oxychloride and phosphorous tribromide proved unsuccessful. However, subjecting **3a-c** to trifluoromethanesulfonic anhydride (Tf$_2$O) in the presence of pyridine in CH$_2$Cl$_2$ yielded exclusively *O*-triflated AQMs **4a-c** in high yields—except in the case of **4c** where the lower yield is ascribed to the poor solubility of the starting material. Subsequent triflate displacement reactions on **4a-c** occur readily in the presence of a variety of neutral nucleophiles including pyridine, 4-(dimethylamino)pyridine, and triphenylphosphine to give iAQMs **5a1-3**, **5b1-2**, and **5c1-2** that can be easily purified after anion exchange. The iAQM compounds are quite soluble in polar organic solvents such as acetone, acetonitrile, DMF, and DMSO, and are stable to further chemical treatment. The bromothiophenylidine derivative **5b1** was further functionalized via Stille coupling to yield **5c1** (Scheme 3a), which is difficult to access via the method used to access the other small-molecule iAQMs. Notably, **5b2** can be polymerized via a mild room-temperature Stille polymerization to yield conjugated polyelectrolytes **P1** and **P2** with ionic groups directly bound to their respective conjugated main chains (Scheme 3b). The AQM conjugated polyelectrolytes were found to display reasonable stability, and did not degrade during normal handling under ambient conditions (Scheme S7 and S8).

Scheme 2. The synthesis of a variety of iAQM small molecules via ditriflate intermediates
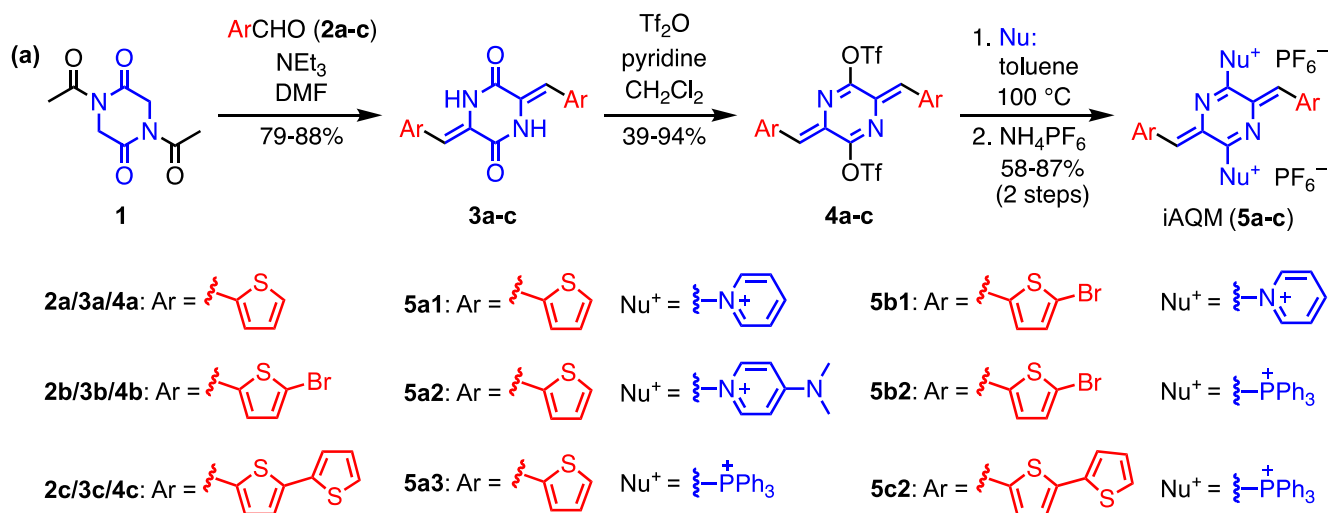
Scheme 3. The synthesis of (a) an extended iAQM small molecule 5c1, and (b) two iAQM CPE via Stille coupling.
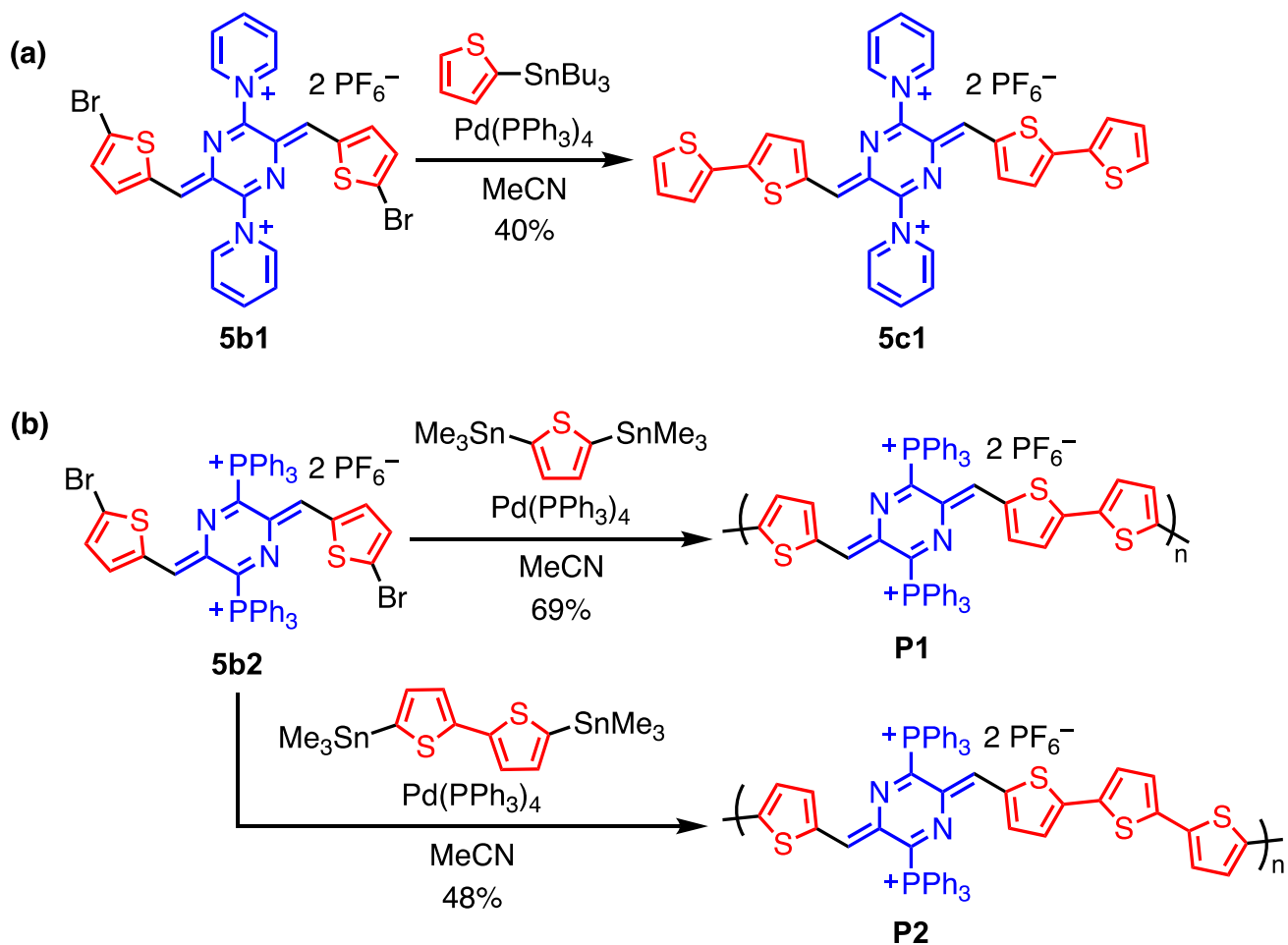
Single-crystal X-ray Structure Analysis

The structures of compounds **5a1**, **5a3**, **5b1**, **5b2** and **5c2** were unambiguously determined by single-crystal X-ray analysis (Figures 1 and S1). In all of the above-mentioned crystal structures, the central AQM ring and the thiophenylidene groups assume a coplanar structure, and the quinoidal nature of the central AQM ring is made clear in the bond length alternation pattern. An S-N interaction is observed in all of the obtained structures except for that of **5c2**, which is presumably disfavored due to steric hinderance. In these structures, the nitrogen atoms of the central AQM ring and the sulfur atoms of the closest thiophene rings face each other with S-N distances significantly shorter (2.898 Å for **5a1** and 2.937 Å for **5a3**) than the sum of the *van der Waals* radii of nitrogen and sulfur atoms (3.35 Å), suggesting a stabilizing interaction. The S-N distances in the iAQMs are all, however, comparatively longer than the S-N distance of 2.800 Å observed in the charge neutral AQM units.[33] The pendant cationic groups in the structures obtained for the iAQMs display consistent geometries wherein the two pyridinium rings in **5a1** and **5b1** are coplanar with each other and offset from the AQM plane by 52° and the triphenylphosphonium units above and below the AQM ring in **5a3**, **5b2**, and **5c2** take on positions 60° offset from each other. None of the salts show π-π stacking in the solid state, presumably due to steric interactions and electrostatic repulsion imposed by the out-of-plane pyridinium and bulky triphenylphosphonium groups (Figure S1). In all cases, each dicationic molecule is paired with two disordered anions—either hexafluorophosphate or trifluoromethanesulfonate—and in some cases is co-crystallized with solvent molecules.
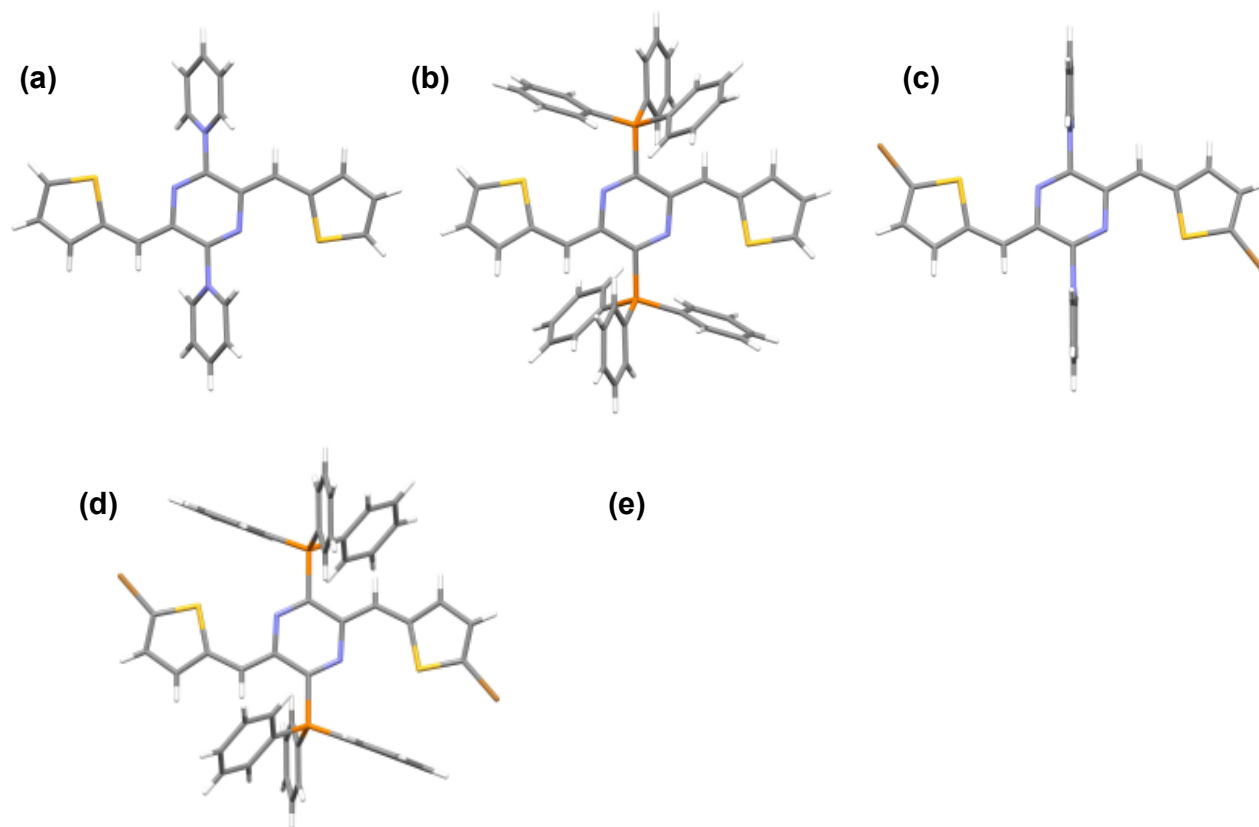
Figure 1. Capped-stick representations of the X-ray structures of (a) **5a1**, (b) **5a3**, (c) **5b1**, (d) **5b2**, and (e) **5c2**. Anions and solvent molecules are omitted for clarity. Note that there is disorder of the outer thiophene units in (e) (see Note after Figure S1).

Optical and Electrochemical Properties

The optical absorption properties of the iAQM small molecules and CPEs are summarized in Table 1 and Figures 2a and S3. The UV-Vis-NIR spectrum of each iAQM small molecule is dominated by a single transition in the visual region — ascribed to the 0–1 π–π* transition, which can be easily shifted via the substitution of either the arylidene group or the cationic substituent. As evinced by the shift in absorption maximum from λ = 526 nm in the case of thiophene-derived **5a3** to λ = 555 nm and 634 nm in the cases of the bromide **5b2** and the bithiophene-derived **5c2**, respectively, both the extension of π-conjugation along the arylidene axis and the introduction of electron-withdrawing groups lead to a red-shift in the absorption. In addition to the main chain conjugation effect, different cationic groups also effectively tune the absorptions. The lowest energy absorption peaks of the

triphenylphosphonium-containing iAQMs **5a3**, **5b2**, and **5c2** show red shifts varying from 18 to 30 nm compared to those of their pyridinium-based counterparts **5a1**, **5b1**, and **5c1**. This is consistent with the fact that the triphenylphosphonium group exert a stronger electron-withdrawing effect than the pyridinium unit (See Figure S3 for additional detail on the small-molecule iAQM absorbances). In addition, the electronic effect of the cationic substituents is demonstrated by comparing the absorption spectra of **5a1** and **5a2**, which differs only by the introduction of an electron-donating dimethylamino group on the pyridinium rings. The absorption maximum of **5a2** (λ = 496 nm) is blue-shifted by about 10 nm compared to that of **5a1** (λ = 505 nm), suggesting a reduced stabilization effect of the LUMO due to increased electron density on the pyridinium rings. iAQM polymers **P1** and **P2** show broad absorbances spanning parts of the visible and NIR portions of the electromagnetic spectrum, with an absorption edge at λ = 1010 nm and 940 nm, respectively. The corresponding optical band gaps are 1.23 eV and 1.32 eV, significantly smaller than that of the monomer **5b2** and the extended oligothiophene derivative **5c2**. Additionally, the band gaps of **P1** and **P2** are also significantly smaller than those previously reported for the neutral AQM polymers, highlighting the greater acceptor character of the iAQM unit.[33] Increasing the number of thiophenes per repeat unit causes a widening in the optical band gap, corroborating the proposal made to explain a similar pattern seen in neutral AQM polymers—dilution of the quinoidal character conferred by the AQM moiety in these polymers.[33] Fluorescence spectroscopy was also performed on the small molecule iAQMs, but no detectable fluorescence was observed (Figure S4). This observation indicates the presence of strong nonradiative deexcitation pathways that quench fluorescence in the iAQMs, possibly releasing the energy instead as vibrational heat.

Table 1. A summary of the relevant data yielded by optical, electrochemical, and computational characterizations of the iAQM compounds reported

Compound	Optical				Electrochemical					Computational		
	λ_{max} (nm)	ε_{max} (L·mol^{-1}·cm^{-1})	λ_{onset} (nm)	E_g (eV)	E_{red} (V)	E_{ox} (V)	HOMO (eV)	LUMO (eV)	E_g (eV)	HOMO (eV)	LUMO (eV)	E_g (eV)

5a1	505	5.75E+04	555	2.23	-0.86	0.80	-5.60	-3.94	1.66	-5.17	-3.22	1.95
5a2	502	4.57E+04	538	2.30	-0.98	0.70	-5.50	-3.82	1.68	-4.76	-2.63	2.13
5a3	526	3.70E+04	587	2.11	-0.84	0.81	-5.61	-3.96	1.65	-4.90	-2.95	1.94
5b1	525	5.82E+04	578	2.15	-0.76	0.84	-5.64	-4.04	1.60	-5.31	-3.39	1.91
5b2	555	5.53E+04	613	2.02	-0.75	0.82	-5.62	-4.05	1.57	-5.12	-3.22	1.90
5c1	616	2.83E+04	696	1.78	-0.80	0.46	-5.26	-4.00	1.26	-4.90	-3.28	1.62
5c2	634	4.11E+04	725	1.71	-0.78	0.50	-5.30	-4.02	1.28	-4.71	-3.19	1.52
P1	806	1.84E+04[a]	1015	1.22	-0.69	0.24	-5.04	-4.11	0.93	--	--	--
P2	768	9.69E+03[a]	933	1.33	-0.71	0.27	-5.07	-4.09	0.98	--	--	--

[a]Calculated assuming that the polymeric material was comprised solely of its repeat unit.

Electrochemical studies of iAQM compounds in solution were carried out using a conventional three-electrode setup and the ferrocene/ferrocenium (Fc/Fc$^+$) redox pair as internal reference. The cyclic voltammetry (CV) traces of each iAQM small molecule and CPE display irreversible oxidation and reduction peaks (Figures 2b and S5), from which an electrochemical band gap and frontier orbital energies can be estimated. As shown in Table 1 and Figure 2c, the electrochemical band gaps of these salts are significantly but consistently smaller than their respective optical band gaps. The LUMO energies obtained electrochemically for the iAQMs are also notably low, indicating the strong electron-withdrawing effect of the ionic groups on the AQM ring. These LUMO values also place the iAQM building block as a notably strong acceptor unit—with the **5a** series displaying significantly lower LUMOs than many other common acceptor units with analogous substitution, with similar values seen in the other iAQMs (Figure S7 and Table S1). The strong accepting nature of the iAQMs stands in stark contrast to the electronics displayed by the charge-neutral AQM small molecules, for which the extrapolated LUMOs are -2.91 and -3.10 eV.[33] This discrepancy may hint that the AQM ring itself is not as strongly accepting as one

may presume based on its structural homology to other strongly accepting motifs, but is readily made into a strong electron accepting unit upon the introduction of electron-withdrawing side groups. CVs of **P1** and **P2** indicate that they may be even stronger electron acceptors than the small molecule iAQMs, and yield electrochemical band gaps reaching below 1 eV, consistent with the trends seen in the optical measurements (Figure 2c and Table 1).
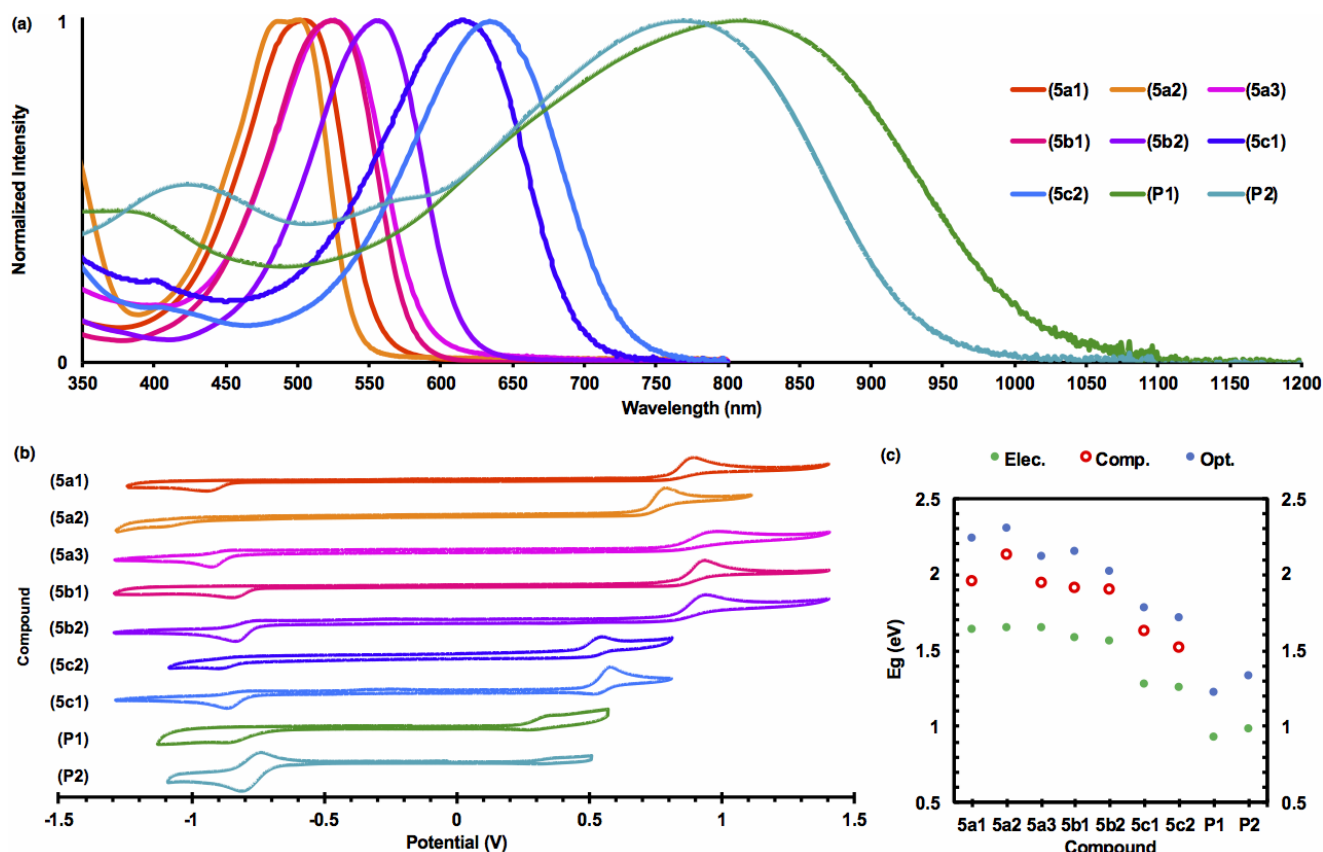

Figure 2. (a) UV-Visible-NIR spectra of iAQM small molecules and polymers. (b) Cyclic voltammograms of iAQM compounds (referenced to the Fc/Fc$^+$ redox couple). (c) A comparison of the band gaps of each iAQM compound obtained experimentally via optical (Opt.) and electrochemical (Elec.) measurements as well as computational (Comp.) predictions thereof.

Theoretical Modeling of Frontier Molecular Orbitals

Density Functional Theory (DFT) calculations were undertaken in order to elucidate the nature of the electronic properties of the small molecule iAQMs. Optimized ground state geometries were established using the 6-31G* basis set for all of the iAQM small molecules, and single-point energy levels were determined using the B3LYP functional at the 6-31G* level with a linear correlation correction.[36] Two chloride anions were included in the calculations as

counter-ions in order to yield reasonable total energies and HOMO/LUMO energy values. Additionally, the geometries of the iAQM small molecules were modeled again after removing the chloride anions in order to visualize the frontier molecular orbitals. The results of these calculations are summarized in Table 1 and Figures 2, 3, S2, and S6. The calculated band gaps of iAQM small molecules consistently fall between the optically and electrochemically predicted gaps, and all three follow a similar trend. However, the calculated frontier energy levels are consistently higher than those of the electrochemically determined levels. Of particular note in the orbital density diagrams is the clear quinoidal nature of the central AQM ring in the HOMO diagram, which is replaced by aromatic character in the LUMO. Additionally, these calculations show clearly that the triphenylphosphonium groups in compounds **5a2**, **5b2**, and **5c2** display little to no orbital density and most likely act solely as strong inductively-withdrawing groups. In contrast, the pyridinium groups in compounds **5a1**, **5b1**, and **5c1** contribute substantially to the LUMO orbital density and may in this way contribute more than just inductively to the energetics of these compounds. Breaking with this trend, the dimethylaminopyridinium group of **5a3** shows little orbital density in its LUMO map, perhaps due to the electron donating effects of the dimethylamino group (Figure S2).

HOMO   LUMO

5a1

5a2

Figure 3. The HOMO and LUMO orbital density maps for iAQMs, **5a1** and **5a2**, modeled without anions and viewed normal to the plane of the AQM ring.

Photothermal Effects

The NIR absorbance of the **P1** and **P2**, along with the lack of fluorescence observed in the small-molecule iAQMs indicated that the iAQM CPEs may perform well as active agents in photothermal therapy. Upon irradiation with an 808 nm laser, solutions of **P1** of different concentrations warmed over time—a necessary property for the application of **P1** as a photothermal therapy agent (Figures 4a and 4b). Higher concentrations of **P1** produced higher temperature solutions the same amount of time under irradiation, with the temperature of water remaining nearly constant over the same irradiation time in the absence of **P1**. A concentration of 30 μM **P1** warmed the solution to 50.6 °C in 5 minutes, a temperature that can cause the death of bacteria through damage to proteins and lipids on the bacterial cell membrane.[37] The extent and speed of warming in such dilute solutions of **P1** indicated that it possesses excellent photothermal properties, thus it was next used as the active agent in

antibacterial photothermal therapy (PTT). Staphylococcus aureus (*S. aureus*), a ubiquitous and dangerous pathogen, was used as a model system for PTT. Photographs of *S. aureus* colonies exposed to different conditions demonstrated that 808 nm laser irradiation alone had little effect on the growth of *S. aureus*, reducing colony count by only 10% (Figures 4c and 4d). Without laser exposure, the application of **P1** solutions (30 µM) caused a 30% colony count reduction, whereas there was a 95% reduction in bacterial colony count after 5 min of 808 nm laser irradiation with **P1**. These results show that **P1** is a strong candidate as an active agent for antibacterial PTT, and also provides one of the first examples of the use of a CPE as an active agent in PTT.
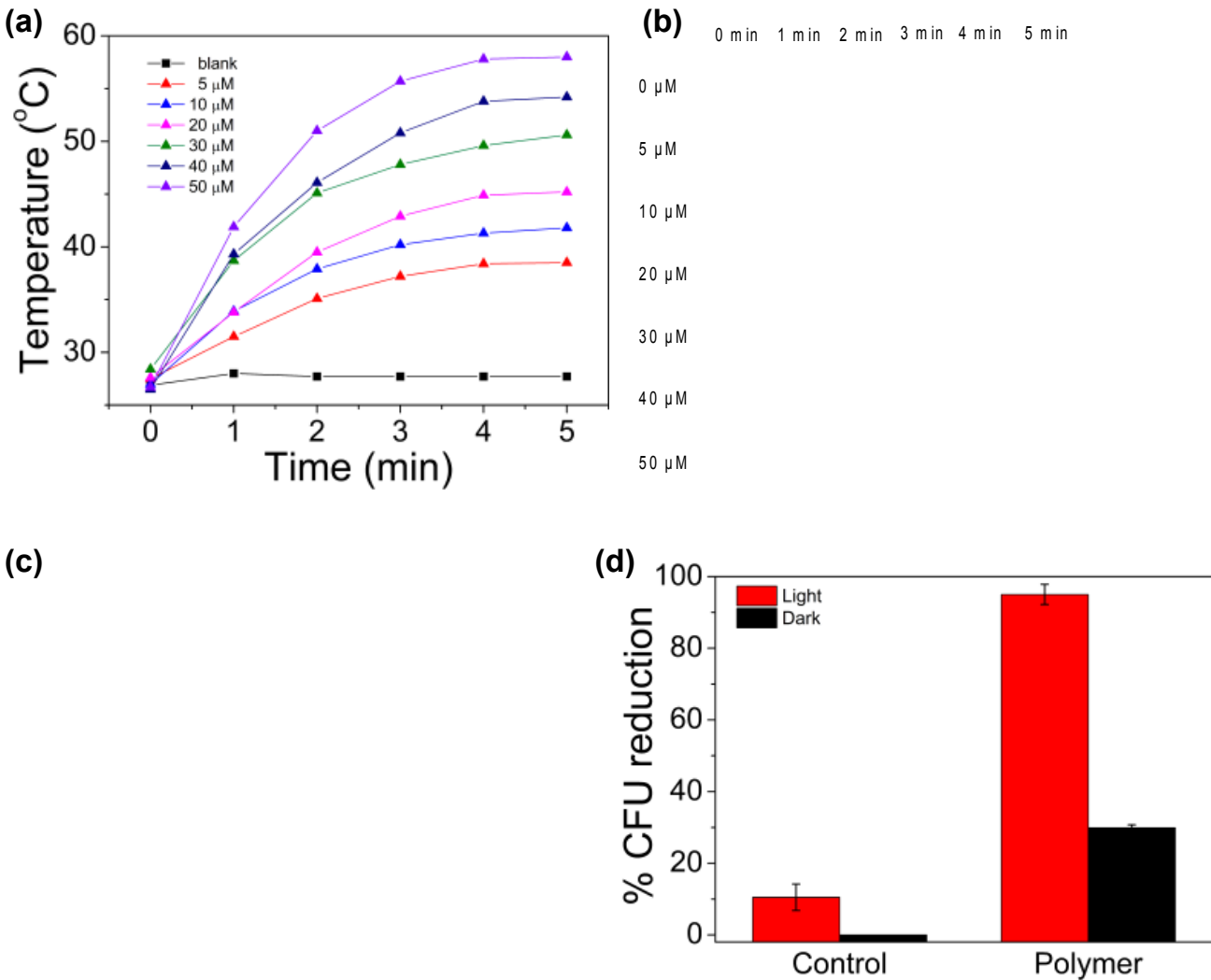
Figure 4. (a) The variation in temperature of aqueous solutions with different concentrations of **P1** over five minutes of irradiation (808 nm laser, 1 W/cm²). (b) IR thermal images of aqueous

solutions with different concentrations of **P1** over five minutes of irradiation (808 nm laser, 1 W/cm^2). (c) Photographs of S. aureus colonies with (**+P1**) and without (**-P1**) exposure to **P1** (30 μM) both with and without laser irradiation for five minutes (808 nm, 850 mW/cm^2). (d) Quantized S. aureus colony reduction data for **P1** with and without 808 nm laser irradiation.

Conclusion

Through this detailed exploration of the iAQM unit—including its synthesis and incorporation into a novel class of low band gap conjugated polymers with applications in photothermal therapy—we have demonstrated the first example of an ionic quinoidal conjugated ring system being used as a building block in low band gap CPEs. The synthesis of the iAQMs presented herein features high overall yields, functional group versatility, as well as the use of low-cost and widely-available reagents. Optical, electrochemical, and theoretical studies revealed that the ionic substituents endow the iAQM molecules with low-lying LUMO energy levels as well as small and highly tunable band gaps. The efficacy shown above in tuning the energetics of a quinoidal conjugated polyelectrolyte system using direct ionic substitution reveals future opportunities in using this strategy to generate more functional ionic semiconductors with desirable optoelectronic properties.

ASSOCIATED CONTENT

Supporting Information

The Supporting Information is available free of charge on the ACS Publications website.

Experimental details and characterization data, as well as additional X-ray structures, frontier molecular orbital density diagrams, UV-Visibile-NIR spectroscopic traces, fluorescence spectroscopic traces, individual cyclic voltammetric traces, and polymer thermal behavior (PDF)

˙Crystallographic data for compound **5a1** (CIF)

Crystallographic data for compound **5a3** (CIF)

Crystallographic data for compound **5b1** (CIF)

Crystallographic data for compound **5b2** (CIF)

Crystallographic data for compound **5c2** (CIF)

AUTHOR INFORMATION

Corresponding Author

yliu@lbl.gov

Author Contributions

The manuscript was written through contributions of all authors. All authors have given approval to the final version of the manuscript.

Notes

The authors declare no competing financial interest.

ABBREVIATIONS

AQM, *para*-azaquinodimethane; iAQM, ionic azaquinodimethane; BLA, bond-length alternation; IR, infrared; HOMO, highest occupied molecular orbital; LUMO, lowest occupied molecular orbital; *p*-QM, *para*-quinodimethane; DDHP, 2,5-dimethylene-2,5-dihydropyrazine; Tf_2O, trifluoromethanesulfonyl anhydride; OTf, trifluoromethanesulfonate or triflate; Fc/Fc^+, ferrocene/ferrocenium redox couple; CV, cyclic voltammetry; UV, ultraviolet; FMO, frontier molecular orbital; DFT, density functional theory; NIR, Near-infrared; PTT, photothermal therapy

REFERENCES

(1)   (a) Cui, Q.; Bazan, G. C. *Acc. Chem. Res.* **2018**, *51*, 202–211. (b) Henson, Z. B.; Zhang, Y.; Nguyen, T. Q.; Seo, J. H.; Bazan, G. C. *J. Am. Chem. Soc.* **2013**, *135*, 4163–4166.

(2)   Mai, C. K.; Zhou, H.; Zhang, Y.; Henson, Z. B.; Nguyen, T. Q.; Heeger, A. J.; Bazan, G. C. *Angew. Chemie - Int. Ed.* **2013**, *52*, 12874–12878.

(3)   Jiang, H.; Taranekar, P.; Reynolds, J. R.; Schanze, K. S. *Angew. Chemie - Int. Ed.* **2009**, *48* (24), 4300–4316.

(4)   (a) Chang, Y.-M.; Leu, C.-Y. *J. Mater. Chem. A* **2013**, *1*, 6446–6451. (b) Liu, Y.; Ogawa, K.; Schanze, K. S. *J. Photochem. Photobiol. C Photochem. Rev.* **2009**, *10*, 173–190.

(5)   Zhu, C.; Liu, L.; Yang, Q.; Lv, F.; Wang, S. *Chem. Rev.* **2012**, *112*, 4687–4735.

(6)   Zhang, K.; Hu, Z.; Xu, R.; Jiang, X. F.; Yip, H. L.; Huang, F.; Cao, Y. *Adv. Mater.* **2015**, *27*, 3607–3613.

(7)   Lee, W.; Seo, J. H.; Woo, H. Y. *Polymer* **2013**, *54*, 5104–5121.

(8)   (a) Xia, R.; Leem, D. S.; Kirchartz, T.; Spencer, S.; Murphy, C.; He, Z.; Wu, H.; Su, S.; Cao, Y.; Kim, J. S.; Demello, J. C.; Bradley, D. D. C.; Nelson, J. *Adv. Energy Mater.* **2013**, *3*, 718–723. (b) Zhou, H.; Zhang, Y.; Mai, C.-K.; Collins, S. D.; Nguyen, T.-Q.; Bazan, G. C.; Heeger, A. J. *Adv. Mater.* **2014**, *26*, 780–785. (c) Zilberberg, K.; Behrendt, A.; Kraft, M.; Scherf, U.; Riedl, T. *Org. Electron.* **2013**, *14*, 951–957. (d) Wu, W.; Bazan, G. C.; Liu, B. *Chem* **2017**, *2*, 760–790. (e) Zhan, R.; Liu, B. *Chem. Rec.* **2016**, *16*, 1715–1740. (f) Pu, K. Y.; Liu, B. *Adv. Funct. Mater.* **2011**, *21*, 3408–3423.

(9)   Seo, J. H.; Gutacker, A.; Sun, Y.; Wu, H.; Huang, F.; Cao, Y.; Scherf, U.; Heeger, A. J.; Bazan, G. C. *J. Am. Chem. Soc.* **2011**, *133*, 8416–8419.

(10)   (a) Rivnay, J.; Inal, S.; Salleo, A.; Owens, R. M.; Berggren, M.; Malliaras, G. G. *Nat. Rev. Mater.* **2018**, *3*, 1–14. (b) Inal, S.; Rivnay, J.; Suiu, A. O.; Malliaras, G. G.; McCulloch, I. *Acc. Chem. Res.* **2018**, *51*, 1368–1376.

(11)   Zeglio, E.; Vagin, M.; Musumeci, C.; Ajjan, F. N.; Gabrielsson, R.; Trinh, X. T.; Son, N. T.; Maziz, A.; Solin, N.; Inganäs, O. *Chem. Mater.* **2015**, *27*, 6385–6393.

(12)   Feng, G.; Mai, C. K.; Zhan, R.; Bazan, G. C.; Liu, B. *J. Mater. Chem. B* **2015**, *3*, 7340–7346.

(13)   (a) Zhou, Z.; Corbitt, T. S.; Parthasarathy, A.; Tang, Y.; Ista, L. K.; Schanze, K. S.; Whitten, D. G. *J. Phys. Chem. Lett.* **2010**, *1*, 3207–3212. (b) Lu, L.; Rininsland, F. H.; Wittenburg, S. K.; Achyuthan, K. E.; McBranch, D. W.; Whitten, D. G. *Langmuir* **2005**, *21*, 10154–10159. (c) Chemburu, S.; Corbitt, T. S.; Ista, L. K.; Ji, E.; Fulghum, J.; Lopez, G. P.; Ogawa, K.; Schanze, K. S.; Whitten, D. G. *Langmuir* **2008**, *24*, 11053–11062. (e) Ding, L.; Chi, E. Y.; Schanze, K. S.; Lopez, G. P.; Whitten, D. G. *Langmuir* **2010**, *26*, 5544–5550. (f) Yuan, H.; Liu, Z.; Liu, L.; Lv, F.; Wang, Y.; Wang, S. *Adv. Mater.* **2014**, *26*, 4333–4338. (g) Zhu, C.; Yang, Q.; Liu, L.; Lv, F.; Li, S.; Yang, G.; Wang, S. *Adv. Mater.* **2011**, *23*, 4805–4810. (h) Zhu, C.; Yang, Q.; Liu, L.; Wang, S. *J. Mater. Chem.* **2011**, *21*, 7905–7912.

(14)   (a) Wallow, T. I.; Novak, B. M. *J. Am. Chem. Soc.* **1991**, *113*, 7411–7412. (b) Rulkens, R.; Schulze, M.; Wegner, G. *Macromol. Rapid Commun.* **1994**, *15*, 669–676.

(15)   (a) Shi, W.; Fan, S.; Huang, F.; Yang, W.; Liu, R.; Cao, Y. *J. Mater. Chem.* **2006**, *16*, 2387–2394. (b) Cimrova, V.; Schmidt, W.; Rulkens, R.; Schulze, M.; Meyer, W.; Neher, D. *Adv. Mater.* **1996**, *8*, 585–588. (c) Colak, D. G.; Cianga, I.; Demirkol, D. O.; Kozgus, O.; Medine, E. I.; Sakarya, S.; Unak, P.; Timur, S.; Yagci, Y. *J. Mater. Chem.* **2012**, *22*, 9293–9300.

(16)   (a) Strakosas, X.; Bongo, M.; Owens, R. M. *J. Appl. Polym. Sci.* **2015**, *132*, 1–14. (b) Nilsson, D.; Robinson, N.; Berggren, M.; Forchheimer, R. *Adv. Mater.* **2005**, *17*, 353–358. (c) Van De Burgt, Y.; Lubberman, E.; Fuller, E. J.; Keene, S. T.; Faria, G. C.; Agarwal, S.; Marinella, M. J.; Alec Talin, A.; Salleo, A. *Nat. Mater.* **2017**, *16*, 414–418.

(d) Gkoupidenis, P.; Schaefer, N.; Garlan, B.; Malliaras, G. G. *Adv. Mater.* **2015**, *27*, 7176–7180.

(17) Rivnay, J.; Owens, R. M.; Malliaras, G. G. *Chem. Mater.* **2014**, *26*, 679–685.

(18) Someya, T.; Bao, Z.; Malliaras, G. G. *Nature* **2016**, *540*, 379–385.

(19) (a) Yuan, Y.; Wang, Z.; Cai, P.; Liu, J.; Liao, L. De; Hong, M.; Chen, X.; Thakor, N.; Liu, B. *Nanoscale* **2015**, *7*, 3067–3076. (b) Feng, G.; Liu, J.; Geng, J.; Liu, B. *J. Mater. Chem. B* **2015**, *3*, 1135–1141.

(20) (a) Geng, J.; Sun, C.; Liu, J.; Liao, L. De; Yuan, Y.; Thakor, N.; Wang, J.; Liu, B. *Small* **2015**, *11*, 1603–1610. (b) Guo, B.; Feng, G.; Manghnani, P. N.; Cai, X.; Liu, J.; Wu, W.; Xu, S.; Cheng, X.; Teh, C.; Liu, B. *Small* **2016**, *12*, 6243–6254.

(21) (a) Shibu, E. S.; Hamada, M.; Murase, N.; Biju, V. *J. Photochem. Photobiol. C Photochem. Rev.* **2013**, *15*, 53–72. (b) Wu, M. C.; Deokar, A. R.; Liao, J. H.; Shih, P. Y.; Ling, Y. C. *ACS Nano* **2013**, *7*, 1281–1290.

(22) Aota, H.; Reikan, T.; Matsumoto, A.; Kamachi, M. *Chem. Lett.* **1997**, *26*, 527–528.

(23) (a) Schnablegger, H.; Antonietti, M.; Göltner, C.; Hartmann, J.; Cölfen, H.; Samorí, P.; Rabe, J. P.; Häger, H.; Walter, H. *J. Colloid Interface Sci.* **1999**, *212*, 24–32. (b) Thünemann, A. F. *Langmuir* **2001**, *17*, 5098–5102. (c) Latini, G.; Parrott, L.; Brovelli, S.; Frampton, M. J.; Anderson, H. L.; Cacialli, F. *Adv. Funct. Mater.* **2008**, *18*, 2419–2427. (d) Subramanyam, S.; Blumstein, A. *Macromolecules* **1991**, *24*, 2668–2674. (e) Bockstaller, M.; Köhler, W.; Wegner, G.; Fytas, G. *Macromolecules* **2001**, *34*, 6353–6358. (f) Bockstaller, M.; Köhler, W.; Wegner, G.; Vlassopoulos, D.; Fytas, G. *Macromolecules* **2001**, *34*, 6359–6366. (g) Thünemann, A. F. *Adv. Mater.* **1999**, *11*, 127–130. (h) Drahomir, V.; Cimrova, V.; Kminek, I.; Pavlackova, P. *Macromol. Symp.* **2010**, *295*, 94–99.
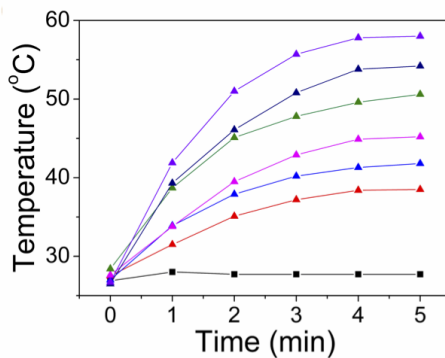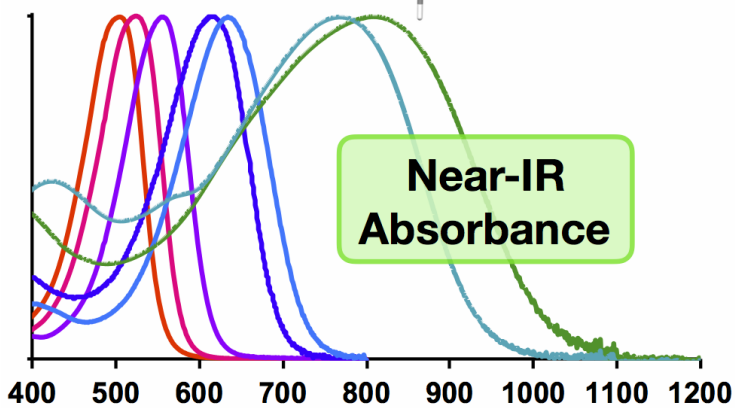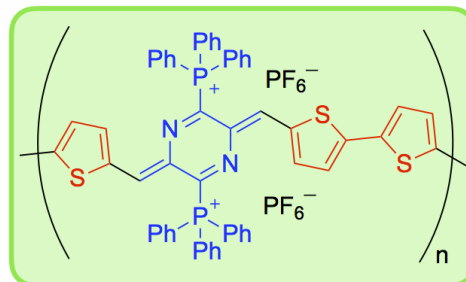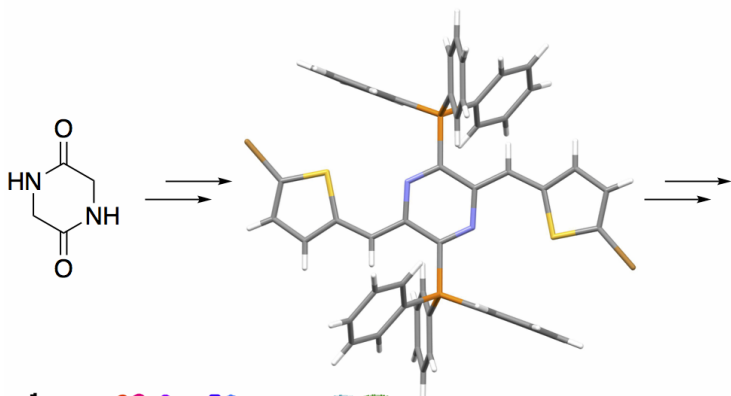
(24)   (a) Klauk, H. *Chem. Soc. Rev.* **2010**, 39, 2643–2666. (b) Lin, Y.; Zhan, X. *Mater. Horizons* **2014**, *1*, 470–488. (c) Ni, W.; Wan, X.; Li, M.; Wang, Y.; Chen, Y. *Chem. Commun.* **2015**, *51*, 4936–4950. (d) Sonar, P.; Fong Lim, J. P.; Chan, K. L. *Energy Environ. Sci.* **2011**, *4*, 1558–1574. (e) Havinga, E. E.; ten Hoeve, W.; Wynberg, H. *Polym. Bull.* **1992**, *29*, 119–126. (f) Havinga, E. E.; ten Hoeve, W.; Wynberg, H. *Synth. Met.* **1993**, *55*, 299–306.

(25)   Ajayaghosh, A. *Chem. Soc. Rev.* **2003**, *32*, 181–191.

(26)   Dou, L.; Liu, Y.; Hong, Z.; Li, G.; Yang, Y. *Chem. Rev.* **2015**, *115*, 12633–12665.

(27)   Kitamura, C.; Tanaka, S.; Yamashita, Y. *Chem. Mater.* **1996**, *8*, 570–578.

(28)   (a) Brédas, J. L. *J. Chem. Phys.* **1985**, *82*, 3808–3811. (b) Wen, L.; Heth, C. L.; Rasmussen, S. C. *Phys. Chem. Chem. Phys.* **2014**, *16*, 7231–7240. (c) Kürti, J.; Surján, P. R.; Kertesz, M. *J. Am. Chem. Soc.* **1991**, *113*, 9865–9867. (d) Hoogmartens, I.; Adriaensens, P.; Vanderzande, D.; Gelan, J.; Quattrocchi, C.; Lazzaroni, R.; Brédas, J. L. *Macromolecules* **1992**, *25*, 7347–7356. (e) Bredas, J. L. *Synth. Met.* **1987**, *17*, 115–121.

(29)   (a) Burrezo, P. M.; Zafra, J. L.; López Navarrete, J. T.; Casado, J. *Angew. Chemie - Int. Ed.* **2017**, *56*, 2250–2259. (b) Casado, J.; Hernandez, V.; Lopez Navarrete, J. T. *Chem. Rec.* **2015**, *15*, 1110–1118.

(30)   Aota, H.; Reikan, T.; Matsumoto, A.; Kamachi, M. *Chem. Lett.* **1997**, *26*, 527–528.

(31)   Meier, H.; Stalmach, U.; Kolshorn, H. *Acta Polym.* **1997**, *48*, 379–384.

(32)   (a) Itoh, T.; Iwasaki, T.; Kubo, M.; Iwatsuki, S. *Polym. Bull.* **1995**, *35*, 307–313. (b) Cram, D. J.; Cram, J. M. *Acc. Chem. Res.* **1971**, *4*, 204–213. (c) Errede, L. A.; Hovt, J. M. *J. Am. Chem. Soc.* **1959**, *82*, 436–439. (d) Hopf, H. Angew. Chemie - Int. Ed. **2008**, 47, 9808–9812. (e) Simon, P.; Mang, S.; Hasenhindl, A.; Gronski, W.; Greiner, A. *Macromolecules* **1998**, *31*, 8775–8780. (f) Gazicki-Lipman, M. *J. Vac. Soc. Japan* **2007**,

50, 601–608. (g) Eiermann, U.; Krieger, C.; Neugebauer, F. A.; Staab, H. A. *Chem. Ber.* **1990**, *123*, 523–533. (h) Eiermann, U.; Krieger, C.; Neugebauer, F. A.; Staab, H. A. *Tetrahedron Lett.* **1988**, *29*, 3655–3658. (i) Eiermann, U.; Neugebauer, F. A.; Symons, M. C. R.; Wyatt, J. L. *J. Chem. Soc. Perkin Trans. 2* **1992**, 91–94. (j) Szwarc, M. Discuss. Faraday Soc. **1947**, 2, 46–49.

(33)   Liu, X.; He, B.; Anderson, C. L.; Kang, J.; Chen, T.; Chen, J.; Feng, S.; Zhang, L.; Kolaczkowski, M. A.; Teat, S. J.; Brady, M. A.; Zhu, C.; Wang, L.; Chen, J.; Liu, Y. *J. Am. Chem. Soc.* **2017**, *139*, 8355–8363.

(34)   (a) Bates, M.; Lunt, R. R. *Sustain. Energy Fuels* **2017**, *1*, 955–968. (b) Young, M.; Suddard-Bangsund, J.; Patrick, T. J.; Pajares, N.; Traverse, C. J.; Barr, M. C.; Lunt, S. Y.; Lunt, R. R. *Adv. Opt. Mater.* **2016**, *4*, 1028–1033. (c) Wessendorf, M. W.; Brelje, T. C. *Histochemistry* **1992**, *98*, 81–85. (d) Frangioni, J. V. Curr. Opin. Chem. Biol. **2003**, 7, 626–634. (e) Escobedo, J. O.; Rusin, O.; Lim, S.; Strongin, R. M. *Curr. Opin. Chem. Biol.* **2010**, *14*, 64–70. (f) Ajayaghosh, A.; Eldo, J. *Org. Lett.* **2001**, *3*, 2595–2598. (g) Chenthamarakshan, C. R.; Eldo, J.; Ajayaghosh, A. *Macromolecules* **1999**, *32*, 5846–5851. (h) Smits, E. C. P.; Setayesh, S.; Anthopoulos, T. D.; Buechel, M.; Nijssen, W.; Coehoorn, R.; Blom, P. W. M.; De Boer, B.; De Leeuw, D. M. *Adv. Mater.* **2007**, *19*, 734–738.

(35)   (a) Yang, L.-M.; Wu, R.-Y.; McPhail, A. T.; Yokoi, T.; Lee, K.-H. *J. Antibiot. (Tokyo).* **1988**, *41*, 488. (b) Gallina, C.; Liberatori, A. *Tetrahedron* **1974**, *30*, 667–673. (c) Bolognesi, M. L.; Tran, H. N. A.; Staderini, M.; Monaco, A.; López-Cobẽas, A.; Bongarzone, S.; Biarnés, X.; López-Alvarado, P.; Cabezas, N.; Caramelli, M.; Carloni, P.; Menéndez, J. C.; Legname, G. *ChemMedChem* **2010**, *5*, 1324–1334. (d) Yokoi, T.; Yang, L.-M.; Yokoi, T.; Wu, R.-Y.; Lee, K.-H. *J. Antibiot. (Tokyo).* **1988**, *41*, 494–501.

(36)   Liu, Y.; Ogawa, K.; Schanze, K. S. *J. Photochem. Photobiol. C Photochem. Rev.* **2009**, *10*, 173–190.

(37)   Feng, G.; Mai, C. K.; Zhan, R.; Bazan, G. C.; Liu, B. *J. Mater. Chem. B* **2015**, *3*, 7340–7346.